Analytica Chimica Acta 1060 (2019) 79–87

Contents lists available at ScienceDirect

Analytica Chimica Acta

journal homepage: www.elsevier.com/locate/aca

Duplex featured polymerase-driven concurrent strategy for detecting of ATP based on endonuclease-fueled feedback amplification

Jingfeng Wang [a], Yu Wang [a], Su Liu [b], Haiwang Wang [a], Xue Zhang [a], Xiaolei Song [b], Jiadong Huang [a, c, *]

[a] College of Biological Sciences and Technology, University of Jinan, Jinan, 250022, PR China
[b] College of Water Conservancy and Environment, University of Jinan, Jinan, 250022, PR China
[c] Key Laboratory of Chemical Sensing & Analysis in Universities of Shandong, College of Chemistry and Chemical Engineering, University of Jinan, Jinan, 250022, PR China

HIGHLIGHTS

- The developed biosensor is based on dual-functional polymerase-driven concurrent strategy termed Endo IV-fueled feedback amplification.
- The G-quadriplex/NMM is used for establishing cost-effective label free biosensor platform.

GRAPHICAL ABSTRACT

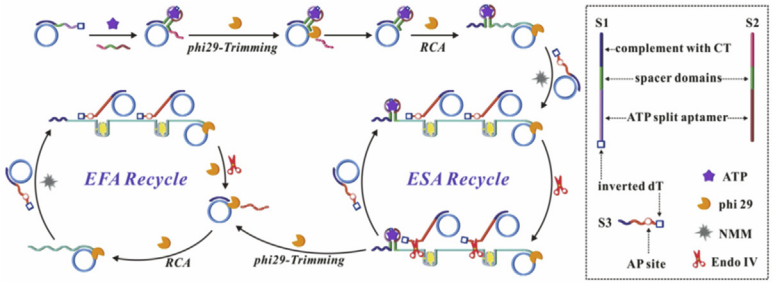

ARTICLE INFO

Article history:
Received 9 October 2018
Received in revised form
11 January 2019
Accepted 23 January 2019
Available online 2 February 2019

Keywords:
Adenosine triphosphate
Split aptamer
RCA
Fluorescence

ABSTRACT

We have developed a novel amplification strategy termed Endo IV-assisted feedback amplification (EFA) taking advantages of rolling circular amplification (RCA) and Endo IV-assisted signal amplification (ESA) biosensing platform for detecting of adenosine triphosphate (ATP). Two kinds of specially programmed DNA complexes were employed into EFA system, one composed of a split aptamer fragment and a circular template, and the other composed of AP probe and the same circular template. Hence, ATP as a target induced the self-assembly of spilt aptamer fragments and initiated RCA reaction generating a linear DNA, which consists of hybridization elements with Complex II and formation elements of G-quadruplex. More importantly, the addition of endonuclease IV can cut the Complex II into two parts, and one of which can be trimming by phi29 DNA polymerase initiating the new round of RCA reaction producing more RCA products. Thus significantly enhanced fluorescent signal can be measured for ATP as expected, and our proposed strategy exhibits improved performances toward ATP ultrasensitive detection with a limit of detection (LOD) as low as 0.09 nM. Additionally, our developed biosensor demonstrates high selectivity and the superiority of simplicity towards ATP. Above these significant aspects, our proximity binding-induced RCA reaction-based fluorescent assay and Endo IV-fueled feedback signal amplification strategy presents an optimal detection performance towards ATP for potential application in related research and clinical diagnosis.

* Corresponding author. College of Biological Sciences and Technology, University of Jinan, Jinan, 250022, PR China.
E-mail address: chm_huangjd@ujn.edu.cn (J. Huang).

https://doi.org/10.1016/j.aca.2019.01.047
0003-2670/

1. Introduction

Aptamers represent artificial DNA or RNA oligonucleotides-based biorecognition elements originated from an in vivo selection technique termed systematic evolution of ligands by exponential enrichment (SELEX) [1,2]. Typically, aptamers can bind against a wide variety of targets from small organics to large proteins and even cells with controllable high specificity and affinity. Therefore, aptamers are widely used as highly promising pools for biosensors (i.e., aptasensors), molecular devices and therapeutic agents due to their chemically stability, easy availability with high reproducibility, which offer the possibility of overcoming the limitations of antibodies [3,4]. Actually, several aptamers can be split into two moieties that retain biorecognition activity accompanied with target-induced assembly such as aptamer for adenosine triphosphate (ATP). The presence of target ATP can drive the equilibrium toward the formation of two halves of a single aptamer to be a complex with high affinity [5,6]. In this work, the aptamer split into two segments as a recognition element based on proximity binding displayed exceptionally high affinity and specificity toward target ATP.

ATP is considered to be the significant energy source powers related with regulating diverse biological pathway and playing crucial roles in mediating extracellular signaling in living organisms [7]. The level of ATP in human is directly related to diverse important diseases such as Parkinson's disease, malignant tumors and Alzheimer's diseases [8,9]. Considering the significant biological functions of ATP as an indicator in the human body, various strategies have been reported for the detection of ATP such as mass spectrometry, high performance liquid chromatography [10,11]. In order to overcome the shortcoming of time-consuming, poor repeatability and low sensitivity in wide application, the establishment of biosensor platform for high sensitive detection of ATP is of essential significance. Among the biosensing technologies, fluorescence methods are generally recognized as the perfect candidates for widespread application due to the advantages of rapidness, accuracy, high efficiency and sensitivity compared with electrochemical and colorimetric methods [12–16]. Recently, fluorescence-based biosensor with free-labeled assay featuring more precise and cost-efficient than dually-labeled fluorescence probe, using a fluorophore like *N*-methyl mesoporphyrin IX (NMM) and Thioflavin T (ThT) characterized by a promounced structural selectivity for G-quadruplexes. It displays weakly fluorescent by themselves, but exhibits an attractive fluorescence signal enhancement upon binding to DNA G-quadruplexes [17,18].

In addition, the advances in molecular programming have yielded several DNA circuits namely as isothermal amplification technologies for amplifying and improving the detection sensitivity, such as the strand displacement amplification (SDA) [19,20], the loop-mediated isothermal amplification (LAMP) [21,22], rolling circular amplification (RCA) [23,24], and so on. Satisfactorily, RCA reaction can achieve an approximately linear amplification of three to four orders of magnitude, owing to the excellent continuous synthesis characteristics of DNA polymerase [25–27]. Particularly, the DNA polymerases like phi29 DNA polymerase play an important role in improving the high replication performance of RCA reaction, elongating a short DNA primer around a DNA circular template round by round and generating a long single-stranded DNA (ssDNA) with tandem sequence repeats. It's worth noting that phi29 DNA polymerase still exhibits a special function of the processive 3'-5' exonuclease activity, which featuring a marked preference for correction of mismatched base versus a correctly paired 3′ terminus [28,29]. In previous reports, a signal amplification strategy termed DNAzyme feedback amplification (DFA) that takes advantage of RCA reaction and an RNA-cleaving DNAzyme has been developed. RCA reaction was initiated by target to produce enzyme-cleaved elements that converting more probes into triggering the new round of RCA reaction [30,31].

Herein, we have developed a fluorescence-based biosensor strategy that takes advantage of RCA reaction and Endo IV-assisted feedback amplification (EFA) through a cross-feedback mechanism for ultrasensitive detection of ATP. In our proposed strategy, there are several aspects discussing in greater detail below. Firstly, target ATP can bring the corresponding two spilt segments of the aptamer into close proximity, enabling a simultaneous binding. Therefore, the increase of DNA elements local concentrations favors the hybridization of the separate DNA probe (S1 and S2), which are otherwise unable to hybridize spontaneously. Meanwhile, it also allows one portion of S2 to hybridize with the circular template based on the principle of proximity binding above. Secondly, the special structure formed by the linked-affinity ligands of the target, resulting the 3' terminus of the pre-primer mismatched exposed and digested by phi29 DNA polymerase. Then the trimming reactions suspend until the remaining part can be totally converted into a mature RCA primer, triggering the primary RCA reaction and producing primary RCA product. Subsequently, the addition of the Complex II containing an apurinic/apyrimidinic (AP site) can bind with the primary RCA product. At the same time, RCA products contain G-rich sequences, forming G-quadruplex. When the NMM is bound to G-quadruplex, the strong interaction between the activated G-quadruplex and NMM generating a significant fluorescence signal enhancement compared with the NMM itself. Thirdly, the primary RCA product as a very long ssDNA consists of tandem repeated DNA segments binding with the Complex II forming duplex DNA containing the AP sites, which is nicked by Endo IV-catalyzed cyclic cleavage reaction with the unique superiority of high efficiency and straightforward operation. Subsequently, two sections of the Complex II fell off the RCA products, and then more mature primers were generated through the trimming reaction by phi29 DNA polymerase and fed back into the new round of RCA reaction. Therefore, the Complex II played a significant role in achieving the EFA system and improving the detection sensitivity, enabling ultrasensitive detection of ATP with a limit of detection (LOD) as low as 0.09 nM. In terms of these aspects above, our proximity binding-induced RCA reaction-based fluorescent assay and Endo IV-assisted feedback signal amplification strategy may establish a robust and efficient biosensor platform for ultrasensitive detection of ATP.

2. Experimental section

2.1. Materials and reagents

All sequences of which oligonucleotides listed in Table 1 were HPLC-purified and synthesized by Sangon Biotechnology Co. Ltd. (Shanghai, China). ATP, GTP, CTP, UTP, endonuclease IV (Endo IV), T4 DNA ligase, 10 × T4 DNA ligase reaction buffer (50 mM Tris-HCl, 10 mM $MgCl_2$, 10 mM DTT, 1 mM ATP, pH 7.5), *E.coli* exonuclease I (Exo I), *E.coli* exonuclease III (Exo III), phi29 DNA polymerse, 10 × phi29 DNA polymerse reaction buffer (50 mM Tris-HCl, 10 mM $MgCl_2$, 10 mM $(NH_4)_2SO_4$, 4 mM DTT, pH 7.5), deoxynucleotide (dNTP) solution mix were purchased from New England Biolabs (Ipswich, MA, USA). N-methylmorpholine (NMM) was purchased from Frontier&Scientific (Philadelphia, United States). The stock solution of NMM (24 M) was prepared in dimethyl sulfoxide (DMSO), stored in darkness at −20 °C. The concentration of NMM was measured by UV−vis spectrometer (Shimadzu UV-2600, Japan) and found to be $\lambda = 379$ nm, assuming an extinction coefficient of $1.45 \times 10^5\ M^{-1}\ cm^{-1}$. The agarose and DNA marker (DL15000) were purchased from Takara Biotechnology Co. Ltd. (Dalian, China).

Table 1
DNA oligonucleotides sequence used in this work.

Oligonucleotide name	Sequence (5′ to 3′)
S1	CACACGAATTCATCTGTTTTTTACCTGGGGGAGTAT-Inverted dT
S2	TGCGGAGGAAGGTTTTTTTGGGTATTTTTTTTTTTTACTTTCCTAGC
S3	CACACGAATTCATCTGTTTTTTTTTTTTACTCTTCCTAGCTXACATGGC-Inverted dT
padlock probe	P-ATTCGTGTGTAGCTTACATGGCTTTTCCCAACCCGCCCT ACCCTTTTTAGCTTACATGGCTTTTCCCAACCCGCCCTACCCCAGATGA
ligation probe	CACACGAATTCATCTG

Other chemicals were of analytical grade and were used without further purification. Ultrapure water obtained from a Millipore filtration system was used throughout.

The DNA sequences highlighted in underline in S1 and S2 represented two split aptamer of ATP. The 3′ inverted dT modification in both S1 and S3 can inhibit the digestion of the 3'-5′ exonuclease activity of phi29 DNA polymerase. The P in the linear padlock probe denotes a 5′ phosphate modification. The X highlighted in red is the tetrahydrofuran abasic site mimic (AP site).

2.2. Apparatus

Gel electrophoresis was conducted using DYCZ-24DN electrophoresis cell (LIUYI, Beijing, China) and Bio-Rad Gel imaging system (Bio-Rad, USA). Absorbance spectrum was obtained by UV–vis spectrometer (Shimadzu UV-2600, Japan). Fluorescence spectra were recorded using an Agilent Cary Eclipse spectrofluorometer (Hitachi, Japan) with excitation at 399 nm. The slit was set to be 10 nm for both the excitation and the emission.

2.3. Preparation of circular template

The circular template I was prepared via an intramolecular ligation in an aliquot of 60 μL reaction system containing 6 μL of 100 μM 5'-phosphorylated linear padlock probe, 6 μL of 100 μM ligation probe, 6 μL 10 × T4 DNA ligase reaction buffer (50 mM Tris-HCl, 10 mM $MgCl_2$, 10 mM DTT, 1 mM ATP, pH 7.5) which were added and incubated for initial denaturation at 95 °C for 5 min, then slowly cooled down to room temperature. After that, 3 μL of 400 U μL^{-1} T4 DNA ligase was added and incubated at 16 °C overnight. The ligation reaction solution was terminated by a thermal treatment at 65 °C for 10 min to inactivate the T4 DNA ligase. Subsequently, to digest the free and hybridized probe, 1 μL Exo I, 2 μL Exo III were added to the ligation reaction solution above followed by incubation 2 h at 37 °C. After inactivating at 85 °C for 20 min, the resultant products were stored at 4 °C for further use. Additionally, the circular template II (100 nM) can be obtained by diluting the circular template I (10 μM) 100 times.

2.4. Preparation of complex I and complex II

The Complex I was prepared in an aliquot of 60 μL reaction system containing 6 μL of 100 nM circular template II, 6 μL of 100 nM S1, 12 μL 5 × PBS buffer (10 mM Na_2HPO_4, 10 mM NaH_2PO_4, 140 mM NaCl, 1 mM KCl, 1 mM $MgCl_2$, 1 mM $CaCl_2$, pH = 7.4) which were added and incubated for initial denaturation at 37 °C for 1 h. The Complex II was prepared in an aliquot of 60 μL reaction system containing 30 μL of 10 μM circular template I, 6 μL of 50 μM S3, 12 μL 5 × PBS buffer (10 mM Na_2HPO_4, 10 mM NaH_2PO_4, 140 mM NaCl, 1 mM KCl, 1 mM $MgCl_2$, 1 mM $CaCl_2$, pH 7.4) which were added and incubated for initial denaturation at 37 °C for 1 h.

2.5. ATP-induced proximity-dependent sensing fluorescence assay

The detailed procedure was as follows: 3 μL of 10 nM Complex I prepared above, 3 μL of 5 μM Complex II and 3 μL of 10 nM S2 were added into 30 μL of amplification reaction mixture containing 3 μL 10 × phi29 DNA polymerase reaction buffer (50 mM Tris-HCl, 10 mM $MgCl_2$, 10 mM $(NH_4)_2SO_4$, 4 mM DTT, pH 7.5), 2 μL of 10 mM dNTPs, 3 μL of different concentrations of ATP, 3 μL of 5 U μL^{-1} Endo IV, 3 μL of 10 U μL^{-1} phi29 DNA polymerase, 3 μL of 2.4 μM NMM solution which were incubated at 37 °C for 90 min for ATP-induced proximity binding initiated rolling circular amplification based label-free fluorescence assay. Ultimately, the above reaction solution was mixed with 70 μL of ultrapure water and scanned using Agilent Cary Eclipse spectrofluorometer. Unless noted otherwise, all experiments for ATP measurements were repeated three times in this research.

2.6. Gel electrophoresis

The gel electrophoresis was performed to analyze the ligation reaction products and target-driven RCA reaction products on a 1% agarose gel with a fluorescence stain Cyber Gold (0.5 μg mL^{-1}) in 50 mM Tris-borate running buffer (2 mM EDTA, pH = 8.2) at 145 V for 35 min. Then the gel was visualized via fluorescence detection using a Bio-Rad Gel imaging system after electrophoresis.

2.7. Detection of ATP in real samples

We have spiked different concentrations of ATP (0, 0.1 nM, 1 nM, 10 nM, 100 nM) into the human serum samples and measured directly with a buffer solution in place of no-pretreatment except for dilution (1: 10 dilution ratio between serum and buffer). The human serum samples were collected by centrifugation of whole blood after coagulation.

3. Results and discussion

3.1. Principle of the proposed strategy for ultrasensitive ATP detection

Scheme 1 represents working mechanism of the proposed strategy for ultrasensitive detection of ATP, including the target proximity binding-induced RCA reaction, phi29 DNA polymerase trimming reaction and Endo IV-assisted feedback amplification for fluorescent signal response. The whole system is mainly made of two spilt aptamer of ATP namely as S1 and S2, the circular template (CT), and the ssDNA probe namely S3 containing AP site as the substrate of Endo IV. These DNA elements can be applied ingeniously for the synthesis into two DNA complexes: Complex I formed by hybridization of S1 and circular template, and Complex II formed by hybridization of S3 and circular template. These complexes above trigger the following amplification reactions orderly. First of all, the presence of target ATP can initiate the proximity binding process between two spilt segments of aptamer with high

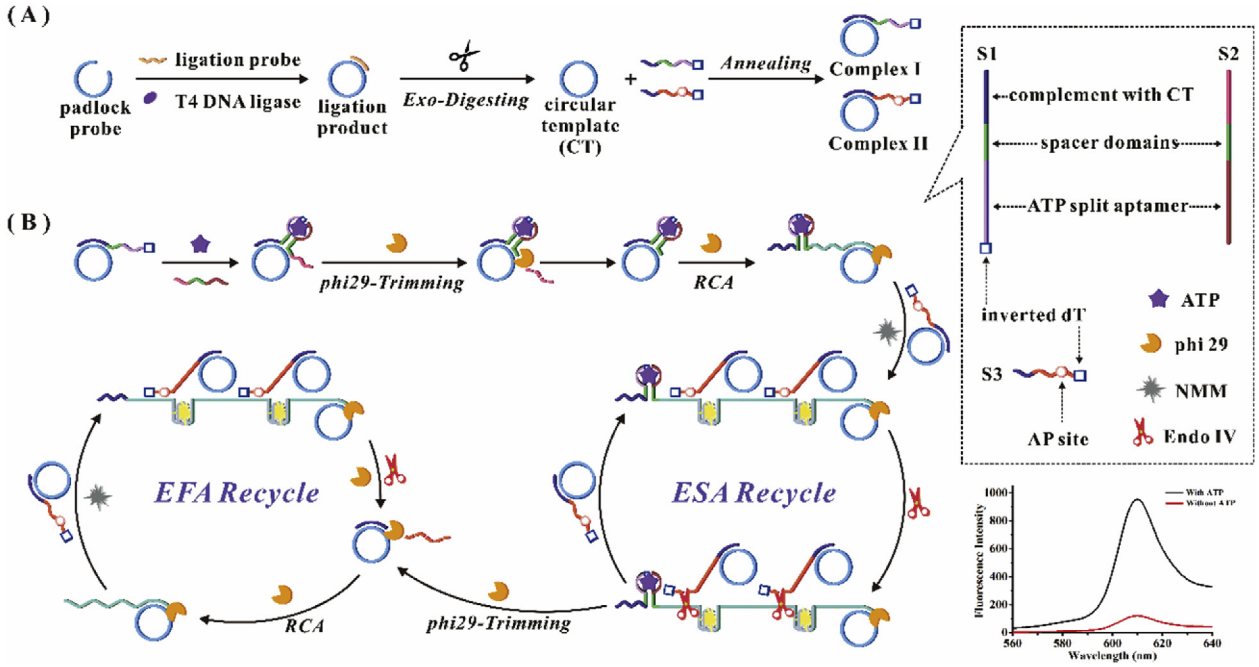

Scheme 1. (A) Synthetic mechanism of circular template and complex probes. (B) Schematic diagram of the label-free fluorescent sensing of ATP based on proximity binding-induced exonucleolytic digestion-assisted primer generation for RCA coupled with Endo IV-assisted signal amplification (ESA) and Endo IV-assisted feedback amplification (EFA).

specificity, inducing the increase of DNA elements local concentrations. Moreover, two separate DNA probes that may not have been hybridized spontaneously can have been hybridized by proximity binding to the target synchronously. Thus, the green portion represents polyT spacer domains in both S1 and S2, aiming to avoid any steric hindrance when two split aptamers binding to the ATP target, can close to each other dynamically, and one part of S2 can hybrid with the circular template, forming a DNA complex structure and leaving a 3′ terminal pre-primers mismatched versus the circular template. The exposed portion (denoted in pink) was skillfully designed, ensuring the unstable hybridization double-stranded DNA (S2-CT) due to the very low melting temperature (Tm~22.3 °C), which could not be the optimal substrate for phi29. Subsequently, with the aid of phi29 DNA polymerase, the hydrolyzation process could be triggered against the excess base due to the feature of 3'-5′ exonucleolytic digestion. Then, RCA reaction on Complex I was carried out after the pre-primers were converted into the mature RCA primer *via* trimming reaction by phi29. Secondly, as a result, the RCA product was obtained containing G-rich sequence folding into a large number of G-quadruplex units, thus generating the obvious fluorescence enhancement of the NMM embedded in G-quadruplex. In the meantime, the 3′ portion of Complex II could bind with the resultant primary RCA product elements containing repeated sequences, resulting in the formation of the duplex DNA (Complex II/RCA product). Thirdly, due to the formation of the duplex DNA, AP site in Complex II could be embedded into double-stranded DNA, which could be recognized and nicked into two fragments by Endo IV. Subsequently, the cleavage fragments dissociated from the RCA product owing to the very low melting temperature, then phi29 DNA polymerase trimmed the unpaired base generating more mature primer/CT hybrids and feeding back into the new round of RCA process. Additionally, the free RCA product could combine with other Complex II again, initiating new cycles of Endo IV-cleavage. Basically, the reactions above termed Endo IV-assisted feedback amplification. Furthermore, in the EFA process, the RCA reaction could enlarge continuously with recycles achieving the exponential signal amplification, and accumulate more G-quadruplexes which could be probed by NMM showing a remarkable fluorescence signal enhancement. Ultimately, the current strategy is to provide a biosensing platform by the combination of the highly efficient rolling circular amplification reaction and the novel Endo IV-assisted feedback amplification process for ultrasensitive detection of ATP based on fluorescence assay.

3.2. Feasibility assay of ATP detection

After constructing the biosensor platform, the viability of proposed strategy for fluorescence assay of ATP was investigated by carrying out the fluorescence emission spectral responses to a series of control experiments. As depicted in Fig. 1, in the presence of ATP, a significantly strong peak at approximately 610 nm could be observed meaning that proximity binding-induced RCA reaction coupled with Endo IV-assisted feedback amplification has been

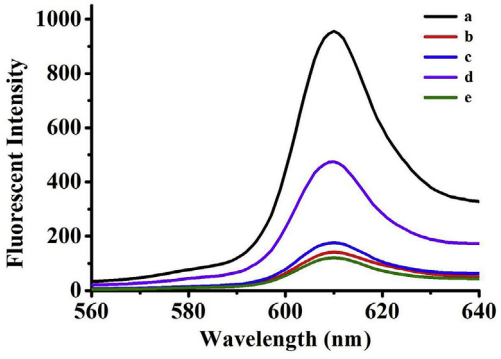

Fig. 1. Fluorescence emission spectra responses of this biosensor obtained upon analyzing 500 nM ATP (curve a). Curves (b to e) are for the feasibility research of the strategy which is controlled with no ATP (curve b), no S2 (curve c), no Endo IV (curve d), non-target ADP in place of ATP (curve e).

successfully performed resulting in the NMM embedded in G-quadruplexes with a remarkably enhanced fluorescence signal (curve a). Contrarily, in the absence of ATP, there was a negligible signal at 610 nm for a blank sample implying that the proximity binding was inhibited with terminated amplification reactions (curve b). Similarly, the fluorescence response almost approximate to that of blank simple in the absence of S2 (curve c), suggesting that the proximity binding-induced hybridization reaction of two spilt aptamers was inhibited and two spilt aptamers played an important role in our proposed strategy. Additionally, a slightly weaker fluorescence intensity was obtained due to the absence of Endo IV (curve d), indicating the Endo IV-assisted feedback amplification was inhibited and the important participation of Endo IV in the whole system. Moreover, an inappreciable fluorescence peak was observed because of the replacement from non-target ADP to target ATP, demonstrating our developed method was carried out by binding of the target and the two spilt aptamers with affinity. These results above clearly show that this biosensor platform providing a feasible method based on fluorescence assay for the detection of ATP.

3.3. Gel electrophoresis characterization

Typically, the preparation of circular template and the rolling circular amplification reaction were verified for straightforward proof *via* gel electrophoresis. Fig. 2 shows the image of gel electrophoresis, and lane 1 displayed the DNA marker (15000 bp). Lane 2 was on behalf of the ligase reaction that the padlock probe could be circularized after hybridization with the ligation probe and specifically ligated with the addition of T4 DNA ligase with a bright band. Similarly, a bright band were obtained after adding Exo I and Exo III with only the circular template remaining (lane 3). On the contrary, no band appeared on the figure after the incubation of padlock probe, ligation probe without T4 DNA ligase, illustrating the two probes were digested by exonuclease (lane 4). It reasonably represented that the circular template was successfully prepared with the aid of several enzymes. As seen from lane 5, a bright band with the large-molecule-weight product and extremely low mobility was appeared on the image, illustrating RCA reaction was commendably implemented and the high efficiency of RCA reaction.

3.4. Function analysis of complex II in EFA system

The fluorescence signal responses mainly came from NMM embedding with G-quadruplexes in RCA products, thus the addition of circular template in Complex probes directly affected RCA reaction efficiency and RCA product concentration. We have investigated the different concentration ratio of Complex II and Complex I through fluorescence assay. As shown in Fig. 3, the $(F-F_0)/F_0$ value gradually enhanced with the increasing of the concentration ratio of both complex probe. Considering the cost value of the S3 composition modification and $(F-F_0)/F_0$ value obtained in the concentration ratio of 1000 times may not be optimal peak, we chose this concentration ratio ($C_{Complex\ II}/C_{Complex\ I} = 500$ times) in subsequent research. Therefore, it can be inferred that

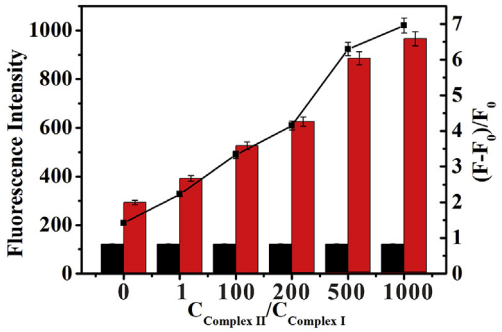

Fig. 3. Effects of the different concentration ratio of Complex II and Complex I on the fluorescence intensity of biosensor. F and F_0 represent the fluorescence emission peak intensity at 610 nm in the presence (the red column) and absence (the black column) of 500 nM ATP. Error bars are standard deviations across thrice repetitive experiments. (For interpretation of the references to color in this figure legend, the reader is referred to the Web version of this article.)

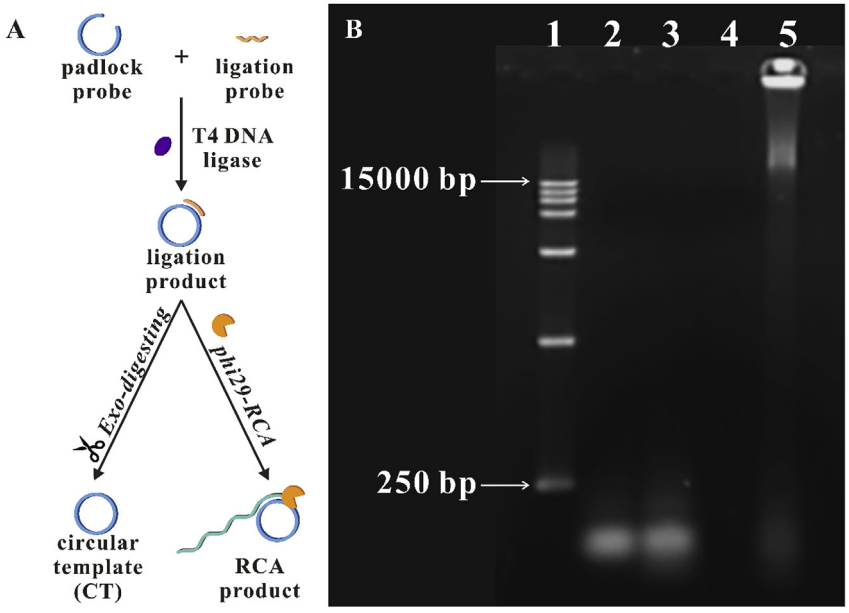

Fig. 2. (A) Principle of the preparation of circular template probe and RCA reaction. (B) Gel electrophoresis image of RCA reaction. Lane 1, DNA marker; Lane 2, padlock probe and ligation probe incubated with T4 DNA ligase; Lane 3, padlock probe and ligation probe incubated with T4 DNA ligase, Exo I, and Exo III; Lane 4, padlock probe and ligation probe incubated with Exo I, and Exo III; Lane 5, RCA products.

Complex II containing AP site is of great importance both on the enhancement of fluorescence responses of the whole EFA system and the continuation of multiple RCA reaction.

3.5. Optimization of experimental conditions

Several experimental conditions including the concentration of Endo IV, phi29 DNA polymerase, NMM and the RCA reaction time have been investigated respectively for confirming the optimum conditions for the biosensor. As shown in Fig. 4, different fluorescence emission peaks were obtained, and it was found that $(F-F_0)/F_0$ value gradually increased upon the increasing of the Endo IV concentration. When the concentration of Endo IV got to 0.5 U μL^{-1}, the fluorescence emission peaks reached equilibrium, thus 0.5 U μL^{-1} was used as the optimal concentration of Endo IV in the subsequent experiments. Additionally, the amount of phi29 DNA polymerase affects the amplified efficiency of the RCA reaction. As depicted in Fig. 4B, the maximum $(F-F_0)/F_0$ value was obtained when the concentration of phi29 reached 1 U μL^{-1} as the optimum concentration. Furthermore, fluorescence emission peaks were produced by the specific binding between NMM and G-quadruplexes so that the concentration of NMM played a vital role in the fluorescence signal enhancement. Fig. 4C shows the maximum $(F-F_0)/F_0$ value at a concentration of 2.4 μM. Typically, the reaction time was extremely an influencing factor of RCA process. As shown in Fig. 4D, the $(F-F_0)/F_0$ value increased upon an increase in the RCA reaction time until a plateau was reached at 90 min tending to be stable. These above results were chosen as the optimal research conditions in the following experiments.

3.6. Analytical performance of our proposed strategy for ultrasensitive ATP detection

Under the optimum experimental conditions research above, the analytical performance of the biosensing platform was further examined by various concentrations of the target ATP using fluorescence spectroscopy. As depicted in Fig. 5A, the current fluorescence responses linearly elevated noticeably with the increasing of the ATP concentration in a range from 0.1 to 500 nM. Fig. 5B shows the linear dependence between the fluorescence intensity at 610 nm and the logarithm of the ATP concentration. It's suggested that our proposed strategy is significant dependent upon the various concentrations of ATP with a linear correlation equation as $F = 204.3 \times LgC + 410.0$ and a correlation coefficient of 0.9954. The limit of detection (LOD) was estimated to be 0.09 nM in terms of three times the standard deviation above the blank signal. Additionally, the sensitivity of our developed biosensor for the detection of ATP was superior compared to several previous methods (Table 2). It's depicted that the sensitivity of our developed fluorescent biosensor is superior to the majority of earlier reported methods mainly including electrochemical and colorimetric assays. Therefore, our proposed strategy presented the advantages of high efficiency and simplified operation for ATP quantification.

3.7. Validation assay of specificity

In order to further examine the selectivity of our proposed strategy, we have measured several fluorescence emissions against target ATP and different non-target molecular including GTP, CTP, UTP as shown in Fig. 6. As expected, the developed biosensor shows a significant current response to the target ATP (500 nM), whereas the diverse responses of the interference molecular (with the concentration 10-fold higher than target) are comparable to that of the blank (in the absence of target ATP). These results above distinctly reveal the high specificity of our proposed strategy for ultrasensitive detection of ATP, and also demonstrate that the spilt segments of aptamer are still valid for binding with ATP.

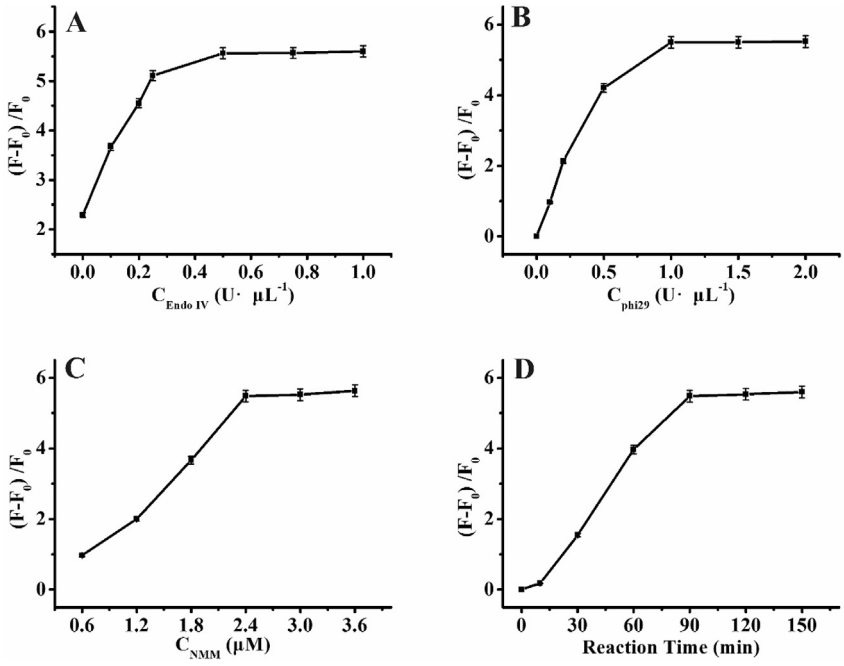

Fig. 4. (A) Effect of the concentration of Endo IV on the fluorescence emission peak of the biosensor. (B) Effect of the concentration of phi29 DNA polymerase on the fluorescence emission peak of the biosensor. (C) Effect of concentration of NMM on the fluorescence emission peak of the biosensor. (D) Effect of RCA reaction time on the fluorescence emission peak of the biosensor. F and F_0 represent the fluorescence emission peak intensity at 610 nm in the presence and absence of 500 nM ATP. Error bars are standard deviations across thrice repetitive experiments.

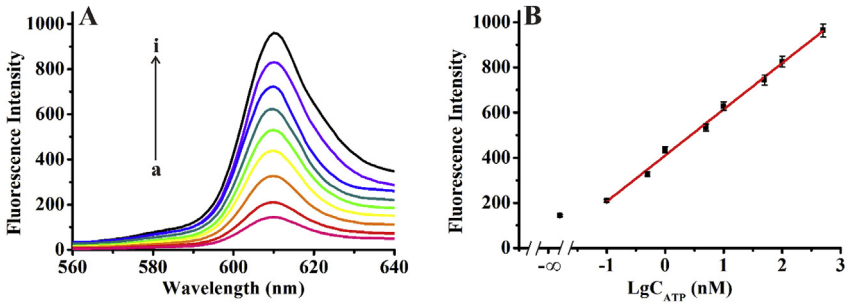

Fig. 5. (A) Fluorescence responses to the different concentrations of ATP (from curve a to i: 0, 0.1 nM, 0.5 nM, 1 nM, 5 nM, 10 nM, 50 nM, 100 nM, 500 nM). (B) The calibration curve of fluorescence intensity at 610 nm for different concentrations of ATP. Error bars are standard deviations across three repetitive experiments. Inset is the plot of the fluorescence intensity at 610 nm versus the logarithm value of ATP concentration.

Table 2
Comparison of different methods for ATP detection.

Detection methods	Detection range (nM)	Detection limit (nM)	Reference
Electrochemical	$1.0–2.0 \times 10^2$	0.6	[32]
Electrochemical	$1.0–1.0 \times 10^2$	0.5	[33]
Colorimetric	$100–5.0 \times 10^3$	61.29	[34]
Colorimetric	$40–4.0 \times 10^3$	40	[35]
Photoelectrochemical	$10–1.0 \times 10^3$	3.2	[36]
Fluorescent	$25–6.0 \times 10^2$	8.2	[37]
Fluorescent	$0.2 \times 10^6–2.2 \times 10^6$	0.3×10^3	[38]
Fluorescent	$0.1 \times 10^5–5.0 \times 10^5$	2×10^3	[39]
Fluorescent	$0.1–5.0 \times 10^2$	0.09	This work

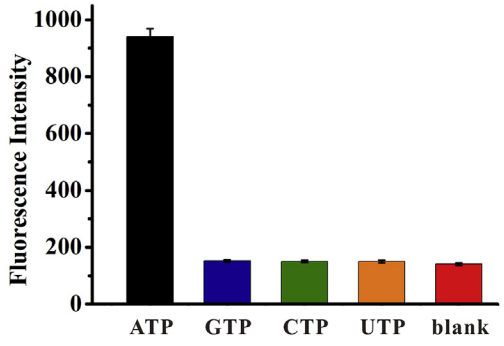

Fig. 6. Plot of the fluorescence intensities at 610 nm obtained upon different molecules. The concentration of ATP is 500 nM. The concentration of the non-target molecules is 5 μM. Error bars are standard deviations across three repetitive experiments.

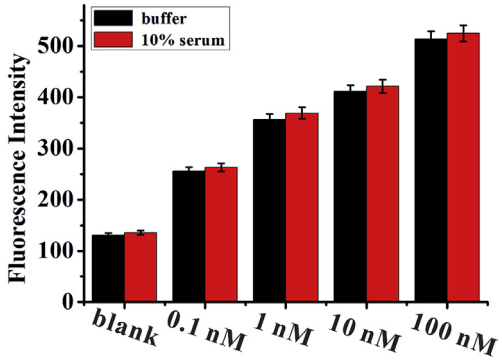

Fig. 7. Plot of fluorescence spectra responses of the developed biosensor for detection of ATP with different concentration in buffer (black bar) and 10% human serum samples (red bar). Error bars are standard deviations across three repetitive experiments. (For interpretation of the references to color in this figure legend, the reader is referred to the Web version of this article.)

3.8. Determination of ATP in actual human serum samples

We have investigated the actual application of our proposed strategy for determination of ATP in real samples. We have chosen the ATP-free human serum samples collected by centrifugation of whole blood after coagulation, of which the mainly composition is similar to the plasma. Thus, we have directly scanned several fluorescence spectra responses upon different concentration of ATP (0, 0.1 nM, 1 nM, 10 nM, 100 nM) as shown in Fig. 7. The fluorescence intensity ascended with the increasing of ATP concentration suggesting that the results obtained in the real samples were in good agreement with those in buffer. The difference between two samples was negligibly smaller than 3.5%, demonstrating that our developed biosensor applied for the detection of ATP in real samples has good accuracy and stability. Additionally, as shown in Table 3, the comparison results between our developed method and high performance liquid chromatography (HPLC) demonstrated the determination results using our strategy was in good agreement with those obtained via HPLC, and the discrepancies between two methods were all smaller than 4.5%. Thus, the developed biosensor may provide a useful method for ultrasensitive detection of ATP in real samples for research upon fundamental biomedicine.

4. Conclusions

In summary, we have successfully developed a rapid and cost-effective label-free fluorescence biosensor for the ultrasensitive detection of ATP. The proposed strategy mainly consists of proximity binding-induced concurrent self-assembly of two split aptamer fragments and cascaded RCA reaction coupled with Endo IV-fueled feedback signal amplification. Intriguingly, phi29 DNA polymerase as a significant fuel has driven concurrent exonuclease-proofreading reaction and polymerase-continuous synthesis

Table 3
Application of developed biosensor for detection of ATP in actual human serum samples and comparison with HPLC method.

Real samples	Spiked amount (nM)	Developed method (±SD, n = 4)	HPLC (±SD, n = 4)
Human serum 1	0.1	0.1044 ± 0.056	0.0997 ± 0.034
Human serum 2	1.0	1.023 ± 0.075	1.015 ± 0.046
Human serum 3	10.0	10.12 ± 0.237	9.896 ± 0.359
Human serum 4	100.0	101.8 ± 0.548	99.57 ± 0.883

reaction. Meanwhile, this cross-feedback mechanism can turn the autonomous transformation of molecular recognition and isothermal amplification technology into possible. Our developed methodology exhibits excellent analytical performance with a limits of detection as low as 0.09 nM and can be extended to a widespread range of biomarkers conveniently with available affinity ligands such as oligonucleotide, protein biomarker and even antigen-antibody. Additionally, our proposed sensing platform has been applied for the detection of ATP in human serum samples. Therefore, the developed strategy may show satisfactory applications in ultrasensitive detection of ATP even other targets such as protein (*e.g.* thrombin, platelet-derived growth factor (PDGF)), other small molecule like cocaine, and possess unlimited potential in drug treatment, disease diagnosis, food safety testing and environmental pollution measuring.

Declaration of interests

☒ The authors declare that they have no known competing financial interests or personal relationships that could have appeared to influence the work reported in this paper.

Acknowledgements

This work was supported by National Natural Science Foundation of China (31471644), the Primary Research & Development Plan of Shandong Province (2017GSF220009, 2016GSF120006).

References

[1] L.C. Bock, L.C. Griffin, J.A. Latham, E.H. Vermaas, J.J. Toole, Selection of single-stranded DNA molecules that bind and inhibit human thrombin, Nature 355 (1992) 564–566.
[2] R. Stoltenburg, C. Reinemann, B. Strehlitz, SELEX–a (r)evolutionary method to generate high-affinity nucleic acid ligands, Biomol. Eng. 24 (2007) 381–403.
[3] S.D. Jayasena, Aptamers: an emerging class of molecules that rival antibodies in diagnostics, Clin. Chem. 45 (1999) 1628–1650.
[4] T. Hermann, D.J. Patel, Adaptive recognition by nucleic acid aptamers, Science 287 (2000) 820–825.
[5] X. Zuo, Y. Xiao, K.W. Plaxco, High specificity, electrochemical sandwich assays based on single aptamer sequences and suitable for the direct detection of small-molecule targets in blood and other complex matrices, J. Am. Chem. Soc. 131 (2009) 6944–6945.
[6] Y. Guo, J. Wu, H. Ju, Target-driven DNA association to initiate cyclic assembly of hairpins for biosensing and logic gate operation, Chem. Sci. 6 (2015) 4318–4323.
[7] X. Zuo, S. Song, J. Zhang, D. Pan, L. Wang, C. Fan, A target-responsive electrochemical aptamer switch (TREAS) for reagentless detection of nanomolar ATP, J. Am. Chem. Soc. 129 (2007) 1042–1043.
[8] A.V. Gourine, E. Llaudet, N. Dale, K.M. Spyer, ATP is a mediator of chemosensory transduction in the central nervous system, Nature 436 (2005) 108–111.
[9] L. Lu, J.C. Si, Z.F. Gao, Y. Zhang, J.L. Lei, H.Q. Luo, N.B. Li, Highly selective and sensitive electrochemical biosensor for ATP based on the dual strategy integrating the cofactor-dependent enzymatic ligation reaction with self-cleaving DNAzyme-amplified electrochemical detection, Biosens. Bioelectron. 63 (2015) 14–20.
[10] Y.-F. Huang, H.-T. Chang, Analysis of adenosine triphosphate and glutathione through gold nanoparticles assisted laser desorption/ionization mass spectrometry, Anal. Chem. 79 (2007) 4852–4859.
[11] Y. Zhou, F. Tozzi, J. Chen, F. Fan, L. Xia, J. Wang, G. Gao, A. Zhang, X. Xia, H. Brasher, W. Widger, L.M. Ellis, W. Zhang, Intracellular ATP levels are a pivotal determinant of chemoresistance in colon cancer cells, Cancer Res. 72 (2012) 304–314.
[12] W. Tedsana, T. Tuntulani, W. Ngeontae, A highly selective turn-on ATP fluorescence sensor based on unmodified cysteamine capped CdS quantum dots, Anal. Chim. Acta 783 (2013) 65–73.
[13] Y. He, J. Tian, K. Hu, J. Zhang, S. Chen, Y. Jiang, Y. Zhao, S. Zhao, An ultrasensitive quantum dots fluorescent polarization immunoassay based on the antibody modified Au nanoparticles amplifying for the detection of adenosine triphosphate, Anal. Chim. Acta 802 (2013) 67–73.
[14] X. Gong, J. Li, W. Zhou, Y. Xiang, R. Yuan, Y. Chai, Target recycling amplification for label-free and sensitive colorimetric detection of adenosine triphosphate based on un-modified aptamers and DNAzymes, Anal. Chim. Acta 828 (2014) 80–84.
[15] T. Bao, H. Shu, W. Wen, X. Zhang, S. Wang, A sensitive electrochemical aptasensor for ATP detection based on exonuclease III-assisted signal amplification strategy, Anal. Chim. Acta 862 (2015) 64–69.
[16] Z.H. Bai, G.Y. Li, J.T. Liang, J. Su, Y. Zhang, H.Z. Chen, Y. Huang, W.G. Sui, Y.X. Zhao, Non-enzymatic electrochemical biosensor based on Pt NPs/RGO-CS-Fc nano-hybrids for the detection of hydrogen peroxide in living cells, Biosens. Bioelectron. 82 (2016) 185–194.
[17] L. Wang, X. Yan, X. Su, A label-free and sensitive fluorescent assay for one step detection of protein kinase activity and inhibition, Anal. Chim. Acta 935 (2016) 224–230.
[18] H.-X. Jiang, Z.-Z. Liang, Y.-H. Ma, D.-M. Kong, Z.-Y. Hong, G-quadruplex fluorescent probe-mediated real-time rolling circle amplification strategy for highly sensitive microRNA detection, Anal. Chim. Acta 943 (2016) 114–122.
[19] N. Zhang, X.-M. Shi, H.-Q. Guo, X. Zhao, W.-W. Zhao, J.-J. Xu, H.-Y. Chen, Gold nanoparticle couples with entropy-driven toehold-mediated DNA strand displacement reaction on magnetic beads: toward ultrasensitive energy-transfer-based photoelectrochemical detection of miRNA-141 in real blood sample, Anal. Chem. 90 (2018) 11892–11898.
[20] M. Jiao, G. Jie, L. Tan, S. Niu, AgNPs-3D nanostructure enhanced electrochemiluminescence of CdSe quantum dot coupled with strand displacement amplification for sensitive biosensing of DNA, Anal. Chim. Acta 983 (2017) 166–172.
[21] W. Du, J. Li, F. Xiao, R. Yu, J. Jiang, A label-free and highly sensitive strategy for uracil-DNA glycosylase activity detection based on stem-loop primer-mediated exponential amplification (SPEA), Anal. Chim. Acta 991 (2017) 127–132.
[22] Y. Wang, D. Liu, J. Deng, Y. Wang, J. Xu, C. Ye, Loop-mediated isothermal amplification using self-avoiding molecular recognition systems and antarctic thermal sensitive uracil-DNA-glycosylase for detection of nucleic acid with prevention of carryover contamination, Anal. Chim. Acta 996 (2017) 74–87.
[23] E.J. Cho, L. Yang, M. Levy, A.D. Ellington, Using a deoxyribozyme ligase and rolling circle amplification to detect a non-nucleic acid analyte, ATP, J. Am. Chem. Soc. 127 (2005) 2022–2023.
[24] F. Yang, Q. Li, L. Wang, G.-J. Zhang, C. Fan, Framework-Nucleic-Acid-enabled biosensor development, ACS Sens. 3 (2018) 903–919.
[25] W. Zhao, M.M. Ali, M.A. Brook, Y. Li, Rolling circle amplification: applications in nanotechnology and biodetection with functional nucleic acids, Angew. Chem. 47 (2008) 6330–6337.
[26] F.B. Dean, J.R. Nelson, T.L. Giesler, R.S. Lasken, Rapid amplification of plasmid and phage DNA using Phi 29 DNA polymerase and multiply-primed rolling circle amplification, Genome Res. 11 (2001) 1095–1099.
[27] B. Schweitzer, S. Roberts, B. Grimwade, W. Shao, M. Wang, Q. Fu, Q. Shu, I. Laroche, Z. Zhou, V.T. Tchernev, J. Christiansen, M. Velleca, S.F. Kingsmore, Multiplexed protein profiling on microarrays by rolling-circle amplification, Nat. Biotechnol. 20 (2002) 359–365.
[28] M. de Vega, J.M. Lazaro, M. Salas, L. Blanco, Mutational analysis of phi29 DNA polymerase residues acting as ssDNA ligands for 3'-5' exonucleolysis, J. Mol. Biol. 279 (1998) 807–822.
[29] C. Garmendia, A. Bernad, J.A. Esteban, L. Blanco, M. Salas, The bacteriophage phi 29 DNA polymerase, a proofreading enzyme, J. Biol. Chem. 267 (1992) 2594–2599.
[30] M. Liu, Q. Zhang, D. Chang, J. Gu, J.D. Brennan, Y. Li, A DNAzyme feedback amplification strategy for biosensing, Angew. Chem. Int. Ed. 56 (2017) 6142–6146.
[31] Y. Gu, T.-T. Zhang, Z.-F. Huang, S.-W. Hu, W. Zhao, J.-J. Xu, H.-Y. Chen, An exploration of nucleic acid liquid biopsy using a glucose meter, Chem. Sci. 9 (2018) 3517–3522.
[32] X. Li, J. Yang, J. Xie, B. Jiang, R. Yuan, Y. Xiang, Cascaded signal amplification via target-triggered formation of aptazyme for sensitive electrochemical detection of ATP, Biosens. Bioelectron. 102 (2018) 296–300.
[33] X. Zhang, C. Song, K. Yang, W. Hong, Y. Lu, P. Yu, L. Mao, Photoinduced regeneration of an aptamer-based electrochemical sensor for sensitively detecting adenosine triphosphate, Anal. Chem. 90 (2018) 4968–4971.

[34] S. Lu, S. Wang, C. Chen, J. Sun, X. Yang, Enzyme-free aptamer/AuNPs-based fluorometric and colorimetric dual-mode detection for ATP, Sensor. Actuator. B Chem. 265 (2018) 67–74.
[35] L. Zhang, S. Guo, J. Zhu, Z. Zhou, T. Li, J. Li, S. Dong, E. Wang, Engineering DNA three-way junction with multifunctional moieties: sensing platform for bioanalysis, Anal. Chem. 87 (2015) 11295–11300.
[36] X. Zhang, Y. Zhao, S. Li, S. Zhang, Photoelectrochemical biosensor for detection of adenosine triphosphate in the extracts of cancer cells, Chem. Commun. 46 (2010) 9173–9175.
[37] X. Tang, R. Deng, Y. Sun, X. Ren, M. Zhou, J. Li, Amplified tandem spinach-based aptamer transcription enables low background miRNA detection, Anal. Chem. 90 (2018) 10001–10008.
[38] Y. Shen, Q. Tian, Y. Sun, J.-J. Xu, D. Ye, H.-Y. Chen, ATP-activatable photosensitizer enables dual fluorescence imaging and targeted photodynamic therapy of tumor, Anal. Chem. 89 (2017) 13610–13617.
[39] G. Liu, J. Lo, D.-Q. Feng, J.-J. Zhu, W. Wang, Silver nanoclusters beacon as stimuli-responsive versatile platform for multiplex DNAs detection and aptamer- substrate complexes sensing, Anal. Chem. 89 (2017) 1002–1008.